

Standing waves in flow between finite counterrotating cylinders

J. Langenberg and G. Pfister

Institute of Experimental and Applied Physics, University of Kiel, 24098 Kiel, Germany

J. Abshagen

Institute for Marine Research, University of Kiel, 24105 Kiel, Germany

(Received 26 February 2003; published 21 November 2003)

Experimental evidence for standing waves resulting from a supercritical Hopf bifurcation that appears as the first pattern-forming instability in counterrotating Taylor-Couette flow is presented. Depending on the aspect ratio two different types of standing waves, denoted as SW_0 and SW_π , could be observed. Both modes have an azimuthal wave number $m=1$ but differ in symmetry. While for SW_π , a spatiotemporal glide-reflection symmetry could be found, SW_0 is purely spatial reflection symmetric. The transition between the two modes is found to be organized in a cusp bifurcation unfolded by variations of the aspect ratio. The “classical” spiral vortex flow appears in this control parameter regime only as a result of a secondary steady bifurcation from SW_0 . This transition is found to be either subcritical or supercritical. The experimentally observed bifurcation structure has been predicted by theory of Hopf bifurcation to spiral vortex flow in finite counterrotating Taylor-Couette systems.

DOI: 10.1103/PhysRevE.68.056308

PACS number(s): 47.20.Ky, 02.30.Oz, 05.45.-a

INTRODUCTION

Bifurcations play an important role in the organization of complex dynamics in nonlinear systems [1]. In spatially extended nonlinear systems, e.g., hydrodynamic flows, steady or time-dependent patterns often arise from a bifurcation of the basic state [2]. Examples of time-dependent pattern resulting from a Hopf bifurcation of the basic state of a hydrodynamic system can be found in binary mixture convection [3–5], in magnetoconvection [6], in stratified Taylor-Couette flow [7], and in counterrotating Taylor-Couette flow [8–20]. Symmetry and symmetry breaking are crucial in order to determine the solution set close to a bifurcation [21]. Spatially extended nonlinear systems are often assumed to have an $O(2)$ symmetry, i.e., a translational and a reflection symmetry [22]. In case of Hopf bifurcation the presence of $O(2)$ symmetry leads to a complex bifurcation structure. The resulting pattern are either traveling waves (TW) or standing waves (SW) (see, e.g., Ref. [21]).

Boundaries play an important role in physical systems. An example of a hydrodynamic system where physical boundaries qualitatively alter the structure of steady bifurcations compared to predictions from theoretical models assuming $O(2)$ symmetry is Taylor-Couette flow [23]. The influence of boundaries on pattern formation and dynamics in the vicinity of Hopf bifurcation have been studied in binary mixture convection with finite geometries. The presence of end walls introduces so-called “blinking states” and “repeated transients” [4]. Boundaries may also be responsible for breaking the reflection symmetry [24] but as a consequence from the finite extent of a system due to boundaries the translational symmetry is broken. The influence of broken translational symmetry on Hopf bifurcation has been investigated theoretically by Refs. [3,25,26]. As a result of broken translational symmetry the bifurcation structure of Hopf bifurcation is qualitatively altered. Instead of traveling and standing waves that occur in the $O(2)$ -symmetric case two different

types of standing waves appear supercritically from the basic state. According to the theory standing waves result from a superposition of two counterpropagating traveling waves having equal amplitudes and a temporal phase difference of either 0 or π . The standing wave solutions have thus been denoted as SW_0 and SW_π having either a purely spatial reflection symmetry or a spatiotemporal glide-reflection symmetry. Traveling wave type solutions (TW') also exist in case of broken translation symmetry but they arise only supercritically or subcritically from a secondary steady bifurcation of each standing wave solution. These TW' solutions differ from the pure TW which occur in case of Hopf bifurcation in $O(2)$ symmetry.

One of the classical hydrodynamic systems for the study of Hopf bifurcation in basic laminar flow is counterrotating Taylor-Couette flow. This is the flow of a viscous fluid confined in a gap between concentric rotating cylinders. Under the assumption of cylinders with infinite axial height the basic laminar Couette flow has an axial translational and reflection symmetry and an azimuthal rotation symmetry. The flow is thus invariant under the group $O(2) \times SO(2)$ [22,27]. On the basis of linear stability analysis of laminar Couette flow Krueger *et al.* [9] predicted the appearance of nonaxisymmetric time-dependent spiral vortices resulting from a Hopf bifurcation for sufficiently high rotation rates of counterrotating cylinders. Spiral vortices have the form of traveling waves in axial direction and of rotating waves in azimuthal direction.

Geometric parameters of experimental systems are the aspect ratio $\Gamma=L/d$, with gap width $d=r_o-r_i$ and axial height L , and the radius ratio $\eta=r_i/r_o$, with r_i and r_o being the radii of the inner and outer cylinders, respectively. The existence of spiral vortices has been confirmed experimentally by Snyder [10]. This investigation has been performed in an apparatus with different radius ratios $\eta=0.2,0.5,0.8,0.956$ and a minimum aspect ratio $\Gamma \approx 17$. A systematic experimental study of counterrotating Taylor-

Couette flow has been performed by Andereck *et al.* [12] using an apparatus with $\eta=0.883$ and aspect ratios Γ ranging from 20 to 48. They found a huge variety of different flow states but as the first time-dependent pattern appearing in azimuthal Couette flow they observed spiral vortices for a wide range of counterrotation rates. Further investigations on primary instabilities and also on bicritical curves for flow between counterrotating cylinders have been performed numerically and experimentally by Langford *et al.* [13] and Tagg *et al.* [14]. They were able to confirm their numerically obtained stability curves experimentally for a flow with an aspect ratio $\Gamma=30$ [14]. In a significantly shorter experimental system with an aspect ratio $\Gamma=12$ Schulz and Pfister [19] were also able to confirm the numerical calculations of Langford *et al.* [13]. Numerical studies on the transition to spiral vortices and their behavior in the nonlinear regime have been performed numerically by Sanchez *et al.* [16] and Hoffmann *et al.* [18] assuming axial periodicity. Experimentally Tagg *et al.* [20] were also able to observe ribbons that appear subcritically in the nonlinear regime. Ribbons are standing waves in axial direction and rotating waves in azimuthal direction. They may also appear supercritically from Hopf bifurcation in counterrotating Taylor-Couette flow under the assumption of translation symmetry [27] but this transition has not been found experimentally yet.

On the basis of theory of Hopf bifurcation with broken translational symmetry Knobloch and Pierce [28] predicted a qualitatively different bifurcation structure in finite counterrotating Taylor-Couette flow compared to the bifurcation that occurs under the assumption of infinite axial height. According to their theory spiral vortices are replaced by standing waves as the first time-dependent pattern resulting from Hopf bifurcation in azimuthal Couette flow. They found two different types of standing waves denoted as in the general theory SW_0 and SW_π both of which differ in symmetry. While SW_π has a glide-reflection symmetry SW_0 has a pure spatial reflection symmetry. Spiral vortices appear only from a subcritical or supercritical steady bifurcation from each standing wave solution in the nonlinear regime. The specific type of bifurcation depends on the system length. Numerical studies of the effect of finite size for the transition to spiral vortices have been performed by Edwards *et al.* [15] and Czarny *et al.* [17] who found complex flow states in a system of small aspect ratio. However, the standing wave solutions and the bifurcation structure predicted by Knobloch and Pierce [28] have not yet been observed either in experimental work or in numerical studies. The aim of this work is to investigate whether standing wave type solutions predicted by Knobloch and Pierce [28] appear in counterrotating Taylor-Couette flow. Our experimental study on the transition to time-dependent flow is performed in a flow having a smaller aspect ratio than in all previous experimental work.

EXPERIMENTAL SETUP

The experimental Taylor-Couette setup consists of a viscous fluid confined in the gap between two independently rotating concentric cylinders. The inner cylinder is machined from stainless steel having a radius of $r_i=(12.50$

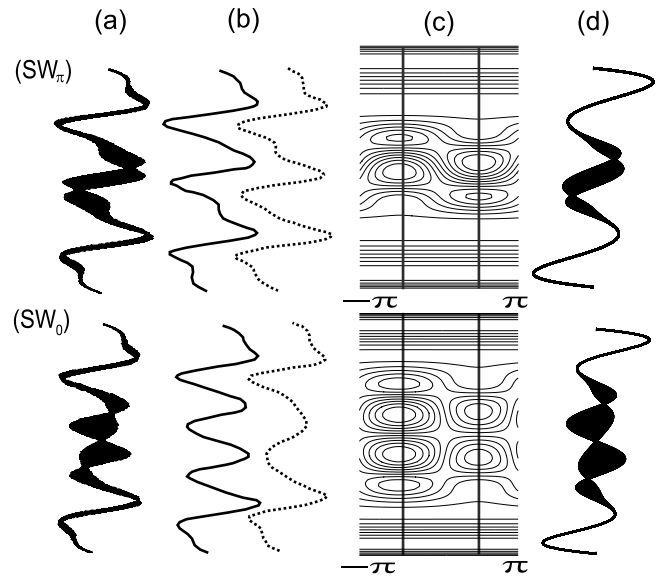


FIG. 1. (a) Axial distributions of axial velocity measured from standing waves SW_π and SW_0 at fixed radial position. (b) Instantaneous axial velocity distributions determined from (a) representing the flow field for an azimuthal phase difference of π . (c) Schematic plot illustrating qualitatively the axial velocity field in axial and azimuthal directions. Vertical lines indicate azimuthal positions corresponding to experimental distributions shown in (b). (d) Schematic plot of axial velocity distributions calculated from (c).

± 0.01) mm, while the outer cylinder is made from optically polished glass with a radius of $r_o=(25.00\pm 0.01)$ mm. As a working fluid silicon oil with the kinematic viscosity $\nu=10.2$ cS is used. The temperature of the fluid is thermostatically controlled to (24.00 ± 0.01) °C. At top and bottom the fluid is confined by end plates which are held fixed in the laboratory frame. The distance between the plates defines the axial height L of the flow which is adjustable within an accuracy of 0.01 mm. The radius ratio is held fixed to $\eta=0.5$ for all measurements and the maximum height of the apparatus is $L=250$ mm which corresponds to a maximum aspect ratio $\Gamma=20$. As control parameters serve the Reynolds number of the inner (i) and the outer (o) cylinders, $Re_{i,o}=dr_{i,o}\Omega_{i,o}/\nu$, where $\Omega_{i,o}$ denote the angular velocity of the inner (i) and the outer (o) cylinders, respectively. We utilize laser doppler velocimetry (LDV) and particle image velocimetry (PIV) for measurements of the flow velocity.

RESULTS

In Fig. 1 characteristic spatial properties of two different time-dependent modes are shown. Both these modes appear as a result of the first time-dependent instability in counterrotating Taylor-Couette flow. The flow states shown in Fig. 1 are measured for $Re_i=114.5$ and $Re_o=-120$ but for different aspect ratios. Spatial properties of one of the modes, labeled SW_π , are depicted in the upper row and of the other mode, labeled SW_0 , in the lower row of Fig. 1. SW_π has been measured in a flow with an aspect ratio $\Gamma=5.7$ and SW_0 in a flow with $\Gamma=6.0$. In Fig. 1(a) experimentally obtained distributions of the axial velocity of SW_π and SW_0 are

presented. They were obtained from LDV measurements of the axial velocity by quasistatic displacement of the measurement volume through the flow in axial direction for a fixed radial position. The appearance of nodal points in both distributions provides strong evidence for standing wave patterns instead of spiral vortices [19]. Note that as the result of fixed end plates an Ekman vortex pattern is also visible in the distributions [29] of axial velocity. Due to flow visualization the azimuthal structure of both SW_0 and SW_π could be identified as that of rotating waves in azimuthal direction having both an azimuthal wave number $m = 1$. From flow visualization it could also be observed that the extrema of the velocity distributions shown in (a) coincide with instantaneous velocity distributions of each flow state. These instantaneous distributions depicted in Fig. 1(b) represent the axial velocity of the standing waves for two different azimuthal positions having a temporal phase difference of π .

According to the theory of Hopf bifurcation with broken translation symmetry standing waves result from a linear superposition of two sinusoidal counterpropagating traveling waves [$\sin(kx + \omega t) + \sin(kx - \omega t + \alpha)$] having equal amplitude but a phase difference $\alpha = 0$ and π for SW_0 and SW_π , respectively. It is observed that the oscillation amplitude goes to zero towards the end. In order to illustrate the appearance of theoretically predicted standing wave solutions in a system with physical boundaries the effect of Ekman vortices and spatial characteristics of the oscillation amplitude has to be taken into account. Schematic diagrams of the axial velocity are depicted in Fig. 1(c) in order to illustrate the axial and azimuthal patterns of SW_0 and SW_π . These flow fields result from a superposition of counterpropagating traveling waves and a qualitative Ekman vortex pattern. As an approximation of the steady Ekman vortices we used an exponentially decaying sinusoidal pattern from each end [29]. The oscillation amplitude in Fig. 1(c) is spatially varying in order to mimic the experimental observations. The resulting pattern corresponding to the vertical lines plotted in Fig. 1(c) is in qualitative agreement with the instantaneous experimental distributions shown in (b). Axial distributions calculated from the pattern shown in (c) are depicted in Fig. 1(d). A strong similarity between (a) measured and (d) calculated distributions can be found.

The most significant difference in the azimuthal structure of the velocity field of SW_0 and SW_π occurs in the axial midplane of the flow. PIV measurements of the (r, z) velocity components in this area shown in Fig. 2 illustrate the azimuthal structure of the velocity field of (a) SW_π and (b) SW_0 . The instantaneous velocity fields were measured with a time lag of $T_0/2$ where T_0 denotes the oscillation period. Due to the rotating wave character of the flow a time lag of $T_0/2$ corresponds to an azimuthal phase shift of π . In coincidence with the azimuthal phase shift of π an axial shift of the flow is observed for SW_π . In contrast to SW_π an alternation between radial inflow and outflow without axial shift with respect to the midplane occurs for SW_0 . Thus SW_0 has a purely spatial reflection symmetry while SW_π has a spatiotemporal glide-reflection symmetries. The symmetries of both experimentally observed standing waves are in agreement with the solutions illustrated in Fig. 1(c).

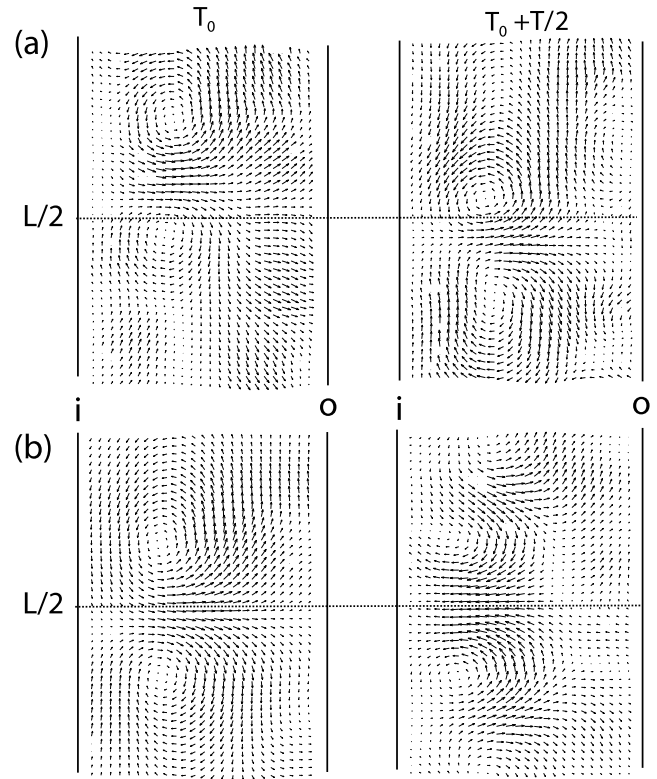


FIG. 2. PIV measurements of instantaneous (r, z) velocity fields obtained from (a) SW_π and (b) SW_0 at $L/2$. Measurements were performed at time difference of $T_0/2$. (T_0 denotes the oscillation period, and i and o the positions of the inner and outer cylinders, respectively.)

In Fig. 3 experimental measurements of two qualitatively different bifurcation diagrams are depicted. The diagrams represent the transition to (a) SW_0 at $\Gamma = 6.0$ and (b) SW_π at $\Gamma = 5.817$ for a fixed outer cylinder Reynolds number $Re_o = -120$. Moreover, in both diagrams the secondary transition from standing waves to spiral vortices (SPI) as well as the oscillation frequency of each time-dependent mode are shown. As a measure of the bifurcations the extrema of the axial velocity component obtained at characteristic measurement points in the flow are used. Due to the reflection symmetry of SW_0 the transitions to these flow states are measured at 5.5 mm above the axial midplane. This is close to the maximum of the oscillation amplitude of SW_0 . Because SW_π and SPI are not reflection symmetric the transition to these flow states is measured in the axial midplane. The radial position of the measurement volume is held fixed at a distance of 1.5 mm from the inner cylinder for all measurements.

In Fig. 3(a) the oscillation amplitude measured at the onset of SW_0 for $\Gamma = 6$ is shown. A square-root law behavior of the amplitude can be seen and has been verified by amplitude fits not shown in the figure. Moreover, the oscillation frequency (\circ) stays constant for increasing Reynolds number having a finite value at onset. This behavior indicates a supercritical Hopf bifurcation to SW_0 at $Re_{SW_0} = 113.2$. In order to represent the transition from SW_0 to SPI a second measurement (\cdot) of the bifurcation scenario is plotted in Fig.

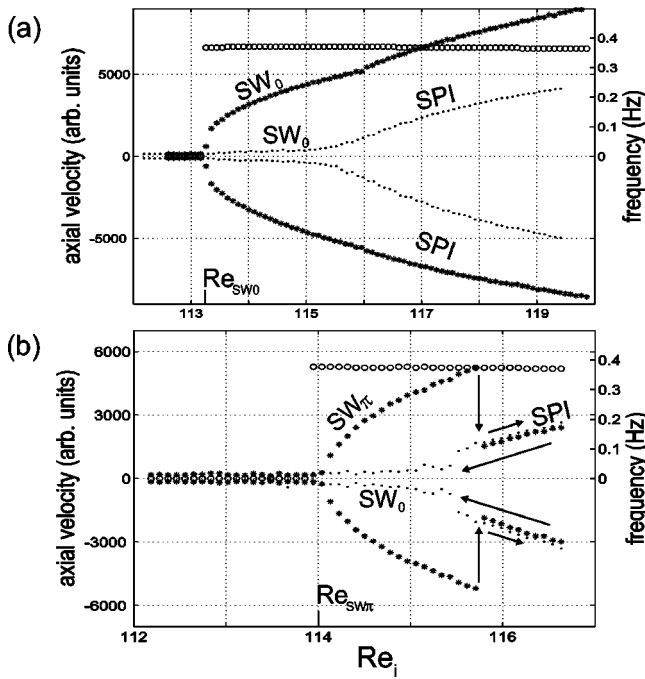


FIG. 3. Experimental measurement of bifurcation diagrams performed at (a) $\Gamma=6.0$ and (b) $\Gamma=5.817$ for $Re_o=-120$. [$(*)$ and (\cdot) represent extrema of axial velocity at measurement position, (\circ) indicates oscillation frequency.] Evidence for supercritical Hopf bifurcation to both (a) SW_0 at $Re_{SW_0}=113.2$ and (b) SW_π at $Re_{SW_\pi}=114.0$ as well as for (a) supercritical and (b) subcritical steady bifurcation to spiral vortices is found.

3(a). In the axial midplane the axial velocity of SW_0 is always zero therefore the amplitude of spirals is clearly visible. Note that Fig. 3(a) represents two different measurements at different measurement points of the same bifurcation scenario. The oscillation frequency remains constant for this transition. This provides evidence that SPI result at this aspect ratio from a secondary supercritical steady bifurcation from SW_0 at higher Reynolds number.

In Fig. 3(b) measurements of the bifurcation scenario for counterrotating Taylor-Couette flow at $\Gamma=5.817$ are presented. The path from the basic state to SPI is indicated by $(*)$ while the reverse path from SPI to the basic state is represented by (\cdot) . The oscillation frequency (\circ) remains constant for the time-dependent modes that occur in the bifurcation sequence. Due to a square-root law behavior of the amplitude and a finite frequency at onset evidence for a supercritical Hopf bifurcation from basic state to SW_π is given. The transition takes place at $Re_{SW_\pi}=114.0$. At higher Reynolds number a transition from SW_π to SPI also occurs for this aspect ratio. In contrast to $\Gamma=6$ the transition to SPI is subcritical as indicated by arrows in Fig. 3(b). As for $\Gamma=6$ a supercritical steady transition between spiral vortices and SW_0 occurs but here it takes place on the secondary branch. A subcritical bifurcation from the secondary branch (SW_0) to the primary branch could also be observed. The bifurcation is found to occur very close to Re_{SW_π} for this particular aspect ratio but in general these two bifurcations do not occur at the same critical Reynolds number. For reasons of

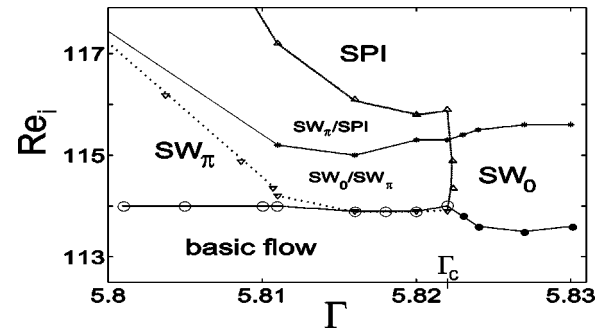


FIG. 4. Experimental stability diagram of counterrotating Taylor-Couette flow for $Re_o=-120$. Solid lines indicate the location of supercritical Hopf bifurcation to SW_0 (\bullet) and SW_π (\circ) and of supercritical steady bifurcation to spiral vortices $(*)$. Dashed lines represent subcritical bifurcation from SW_π (Δ) and from SW_0 (∇) .

clarity we do not present an explicit measurement of the subcritical transition from SW_0 to the basic state in Fig. 3(b).

In Fig. 4 the stability diagram of counterrotating Taylor-Couette flow for $Re_o=-120$ is presented. The bifurcation points were obtained from measurements of bifurcation diagrams as shown in Fig. 3. For $\Gamma < \Gamma_c$ SW_π (\circ) and for $\Gamma > \Gamma_c$ SW_0 (\bullet) are observed as the result of a supercritical Hopf bifurcation. A critical aspect ratio for the Hopf bifurcation is found at $\Gamma_c \approx 5.822$. The stability lines of subcritical bifurcations from SW_π (Δ) and of subcritical bifurcations from SW_0 (∇) form a region of coexistence of the two solutions. Both subcritical stability lines merge within the experimental accuracy with the stability line of the Hopf bifurcation at Γ_c and $Re_i=113.9$. This provides evidence for the existence of a cusp bifurcation between SW_0 and SW_π as a mechanism for stability exchange. Spiral vortices $(*)$ occur in this control parameter regime only supercritically from SW_0 . Note that we found no qualitative and almost no quantitative difference in the bifurcation structure between $\Gamma=5.83$ and $\Gamma=6.0$ shown in Fig. 3(a). For reasons of clarity we have omitted to plot this intermediate region in Fig. 4.

Additional experimental work shows that the appearance of standing waves is not restricted to the aspect ratio regime depicted in Fig. 4. In Fig. 5 two axial velocity distributions (a) of SW_0 measured at $\Gamma=9.0$ and $Re_i=115.1$ and (b) of SW_π measured at $\Gamma=9.5$ and $Re_i=115.0$ are presented. A qualitative similar bifurcation structure could also be observed in this aspect ratio regime. While SW_0 and SW_π still

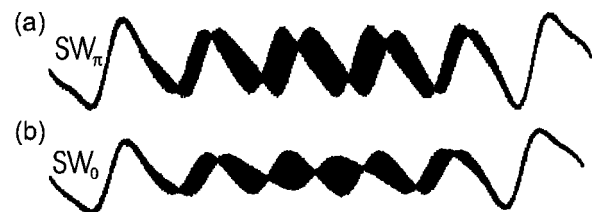


FIG. 5. Axial distributions of axial velocity obtained for $Re_o=-120$ from measurements of (a) SW_π at $Re_i=115.1$ and $\Gamma=9.5$ and of (b) SW_0 at $Re_i=115.0$ and $\Gamma=9.0$.

appear in counterrotating Taylor-Couette flow as a result of supercritical Hopf bifurcation the transition to spiral vortices becomes subcritical. This observation is also in agreement with the theory of spiral vortices in finite cylinders [28].

CONCLUSION

Our work shows, to our knowledge, for the first time experimental evidence for standing wave solutions appearing from a supercritical Hopf bifurcation in counterrotating Taylor-Couette flow. We observe two different types of standing waves which differ in their spatiotemporal symmetries. These standing waves replace spiral vortices as the first time-dependent mode which would appear under the assumption of $O(2)$ symmetry. Spiral vortices appear only as a result of subcritical and supercritical steady bifurcation from standing waves. The observed bifurcation structure has been predicted by theory of Hopf bifurcation in $SO(2) \times O(2)$ symmetric systems where the translational symmetry is broken [28]. The agreement between observations and theory includes not only the appearance of two different types of standing waves having different symmetries but also details such as secondary subcritical or supercritical steady bifurca-

tions to spiral vortices. Experimental evidence is presented that the exchange between the two different standing wave patterns is organized in a cusp bifurcation. This mode exchange is not part of the theory. It shows that for smaller systems in contrast to systems used in previous experimental studies the bifurcation structure depends on the aspect ratio. Thus the aspect ratio is an important control parameter for the transition to spiral vortices in counterrotating Taylor-Couette flow. These results suggest further numerical and experimental works in systems with smaller aspect ratios than used in previous studies. The general conclusion we draw is that important parts of the theory of Hopf bifurcation with broken translation symmetry are applicable to Hopf bifurcation that occurs in experimental systems with physical boundaries.

ACKNOWLEDGMENTS

We thank Wolfgang Schumann and Heinz Horak for their technical support. The authors acknowledge support from the Deutsche Forschungsgemeinschaft. J.L. and G.P. acknowledge support from research Grant No. PF 210/10-1 and J.A. acknowledges support from SFB460.

-
- [1] J. Guckenheimer and P. Holmes, *Nonlinear Oscillations, Dynamical Systems, and Bifurcations of Vector Fields*, AMS 42 (Springer, New York, 1983).
 - [2] M.C. Cross and P.C. Hohenberg, *Rev. Mod. Phys.* **65**, 851 (1993).
 - [3] M.C. Cross, *Phys. Rev. Lett.* **57**, 2935 (1986); *Phys. Rev. A* **38**, 3593 (1988).
 - [4] P. Kolodner, A. Passner, C.M. Surko, and R.W. Walden, *Phys. Rev. Lett.* **56**, 2621 (1986); V. Steinberg, J. Fineberg, E. Moses, and I. Rehberg, *Physica D* **37**, 359 (1986); P. Kolodner, *Phys. Rev. E* **47**, 1038 (1993).
 - [5] W. Barten, M. Lücke, M. Kamps, and R. Schmitz, *Phys. Rev. E* **51**, 5636 (1995).
 - [6] P.C. Matthews and A.M. Rucklidge, *Proc. R. Soc. London, Ser. A* **441**, 649 (1993).
 - [7] F. Caton, B. Janiaud, and E.J. Hopfinger, *Phys. Rev. Lett.* **82**, 4647 (1999).
 - [8] *Physics of Rotating Fluids*, edited by C. Egbers and G. Pfister (Springer, Berlin, 2000).
 - [9] E.R. Krueger, A. Gross, and R.C. Di Prima, *J. Fluid Mech.* **24**, 521 (1966).
 - [10] H.A. Snyder, *Phys. Fluids* **11**, 728 (1968).
 - [11] R.C. Di Prima and H.L. Swinney, in *Hydrodynamic Instabilities and the Transition to Turbulence*, edited by H.L. Swinney and J.P. Gollub, TAP Vol. 45 (Springer, Berlin, 1981).
 - [12] C.D. Andereck, S.S. Lui, and H.L. Swinney, *J. Fluid Mech.* **164**, 155 (1986).
 - [13] W.F. Langford, R. Tagg, E.J. Koestlich, H.L. Swinney, and M. Golubitsky, *Phys. Fluids* **31**, 776 (1987).
 - [14] R. Tagg, W.S. Edwards, H.L. Swinney, and P.S. Marcus, *Phys. Rev. A* **39**, 3734 (1989).
 - [15] W.S. Edwards, R.P. Tagg, B.C. Dornblaser, H.L. Swinney, and L.S. Tuckerman, *Eur. J. Mech. B/Fluids* **10**, 205 (1991).
 - [16] J. Sanchez, D. Crespo, and F. Marques, *Appl. Sci. Res.* **51**, 55 (1993).
 - [17] O. Czarny, E. Serre, P. Bontoux, and R.M. Lueptow, *Theor. Comput. Fluid Dyn.* **16**, 5 (2002).
 - [18] C. Hoffmann and M. Lücke, in *Physics of Rotating Fluids* (Ref. [8]), pp. 55–66.
 - [19] A. Schulz and G. Pfister, in *Physics of Rotating Fluids* (Ref. [8]), pp. 37–54.
 - [20] R. Tagg, W.S. Edwards, and H.L. Swinney, *Phys. Rev. A* **42**, 831 (1990).
 - [21] M. Golubitsky, I. Stewart, and D.G. Schaeffer, *Singularities and Groups in Bifurcation Theory: Vol. 2*, AMS 69 (Springer, New York, 1988).
 - [22] M. Golubitsky and I. Stewart, *SIAM (Soc. Ind. Appl. Math.) J. Math. Anal.* **17**, 249 (1986); M. Golubitsky and W.F. Langford, *Physica D* **32**, 362 (1988).
 - [23] T.B. Benjamin, *Proc. R. Soc. London, Ser. A* **359**, 1 (1978); K.A. Cliffe, J.J. Kobine, and T. Mullin, *ibid.* **439**, 341 (1992); J. Abshagen, O. Meincke, G. Pfister, K.A. Cliffe, and T. Mullin, *J. Fluid Mech.* **476**, 335 (2003).
 - [24] T. Mullin and C. Blohm, *Phys. Fluids* **13**, 136 (2001).
 - [25] E. Knobloch and G. Dangelmayr, *Nonlinearity* **4**, 399 (1991).
 - [26] A.S. Landsberg and E. Knobloch, *Phys. Rev. E* **53**, 3579 (1996).
 - [27] P. Chossat and G. Iooss, *The Taylor-Couette Problem* (Springer, Berlin, 1994).
 - [28] E. Knobloch and R. Pierce, in *Ordered and Turbulent Patterns in Taylor-Couette Flow*, Vol. 297 of *NATO Advanced Studies Institute, Series B: Physics*, edited by C.D. Andereck and F. Hayot (Plenum, New York, 1992).
 - [29] G. Pfister and I. Rehberg, *Phys. Lett. A* **83**, 1 (1981).